Journal of Turbulence
Vol. 00, No. 00, 2009, 1–23

RESEARCH ARTICLE

Analysis of PDFs for Energy Transfer Rates from 4096^3 DNS — Verification of the Scaling Relation within MPDFT —

T. Arimitsu[a*] and N. Arimitsu[b]

[a] *Graduate School of Pure and Applied Sciences, University of Tsukuba, Ibaraki 305-8571, Japan*; [b] *Graduate School of Environment and Information Sciences, Yokohama National University, Yokohama 240-8501, Japan*

(*February 25, 2011*)

The PDFs for energy transfer rates, extracted by Kaneda and Ishihara from their 4096^3 DNS for fully developed turbulence, are analyzed in a high accuracy by means of *multifractal probability density function theory* (MPDFT) in which a new scaling relation has been proposed. MPDFT is a statistical mechanical ensemble theory for the intermittent phenomena providing fat-tail probability density functions (PDFs). With the proposed scaling relation, MPDFT has been improved to deal with intermittency through any series of PDFs with arbitrary magnification δ (> 1). Since the value of δ can be determined freely by observers, the choice of δ should not affect observables. The validity of the generalized MPDFT is verified successfully through the precise analyses of several series of PDFs with different values of δ. In addition to the verification, it is revealed that the system of fully developed turbulence has much wider area representing scaling behaviors than the inertial range. With the help of MPDFT, it has come to possible to separate the coherent turbulent motion from fluctuations, which may benefit the wavelet analysis of turbulence.

Keywords: Multifractal PDF theory; Intermittency; Energy transfer rates; Tsallis-type distribution function; Fat-tail PDF

1. Introduction

The keystone works [1–14] providing the multifractal aspects for fully developed turbulence deal mostly with the scaling property of the system, e.g., comparison among the scaling exponents of velocity structure function. Only a few [8, 12–21] analyze the probability density functions (PDFs) obtained by experiments or numerical experiments. Among the researches analyzing PDFs, multifractal probability density function theory (MPDFT) [12, 13, 15, 16, 18, 19, 21] offers the most precise analyses of the system including PDFs.

MPDFT is a statistical mechanical ensemble theory for analyzing those phenomena providing fat-tail PDFs, which was constructed by the authors under the assumption, following Frisch and Parisi [2], that the singularities due to the scale invariance of the Navier-Stokes (N-S) equation for high Reynolds number distribute themselves multifractal way in real physical space. The degree of singularity for those quantities which are responsible for intermittent phenomena is specified by the singularity exponent α that is assumed to be equal to the parameter appeared in the scale transformation as an arbitrary parameter taking real values (see (10) and (11) below). Note that α is regarded as a stochastic variable, and is related

*Corresponding author. Email: arimitsu.toshi.ft@u.tsukuba.ac.jp

ISSN: 1468-5248 (online only)

DOI: 10.1080/14685240YYxxxxxxx
http://www.informaworld.com

definitely to the quantity representing intermittent behavior. Within the approach of MPDFT, the p model [5], the log-normal model [22–24] and the A&A model [10–13, 15, 16, 18, 19, 21] are categorized as models with increasing number of parameters in the probability density function for α, which are determined self-consistently as functions of the intermittency exponent μ. For the case of the p model, the distribution of α is given by the binomial distribution function with one parameter that is specified by the definition of μ. For the log-normal model, the distribution of α is given by the Gaussian distribution function with two parameters which are determined by the condition for energy conservation and the definition of μ. For the case of the A&A model, the distribution of α is given by Tsallis-type distribution function with three parameters which are fixed by the condition of energy conservation, the definition of μ and the *scaling relation*. The extraction of an appropriate distribution for α may lead us to a resolution for the origin of intermittency in turbulence. MPDFT provides us with a systematic framework to make a connection between the distribution of α and the PDFs of observed quantities. The superiority of A&A model within MPDFT to other theories has been checked by comparing [15] the scaling exponents of the velocity structure function given by the present theory with those by other theories, and furthermore by comparing [18] the PDFs provided by the present model with those by the p-model [5] and by the log-normal model [22–24].

In order to extract the intermittent character of the fully developed turbulence, it is necessary to have information of hierarchical structure of the system. This is realized by producing a series of PDFs for responsible singular quantities with different lengths

$$\ell_n = \ell_0 \delta^{-n}, \quad \delta > 1 \quad (n = 0, 1, 2, \cdots) \tag{1}$$

that characterize the sizes of eddies or the regions in which the physical quantities are coarse-grained. The value for δ is chosen freely by observers. Note that the number of steps n depends on δ, since if one took a smaller value for δ, he would need more steps to reach the same length ℓ_n as before for a fixed value of ℓ_0. Therefore, the choice of δ should not affect the theoretical estimation of the values for the fundamental quantities, i.e., observables characterizing the turbulent system under consideration. The A&A model within the framework of MPDFT itself tells us that this requirement is satisfied if the scaling relation has the form [1]

$$(\ln 2)/(1-q)\ln\delta = 1/\alpha_- - 1/\alpha_+. \tag{3}$$

Here, q is the index associated with the Rényi entropy [27] or with the Havrda-Charvat [28] and Tsallis [29] (HCT) entropy; $\alpha_\pm$ are zeros of the multifractal spectrum (see below in sub-section 4.1). The multifractal spectrum is uniquely related to the PDF for α which is responsible for the tail part of PDFs for those quantities revealing intermittent behavior whose singularity exponents can have values $\alpha < 1$. With the new scaling relation (3), observables have come to include the parameter δ only in the combination $(1-q)\ln\delta$. The difference in δ is absorbed in the entropy index q.

[1] Since almost all the PDFs that had been provided previously were for the case where $\delta = 2$, it has been possible to analyze PDFs with the scaling relation

$$1/(1-q) = 1/\alpha_- - 1/\alpha_+ \tag{2}$$

proposed by Costa, Lyra, Plastino and Tsallis [25, 26] in the context of dynamical systems.

This generalization of the scaling relation naturally leads us to replace n appeared in the Tsallis-type distribution function (see (45) below) within A&A model with a new number

$$\tilde{n} = n \ln \delta. \tag{4}$$

Then, the PDF of α becomes δ independent if the new number $\tilde{n}$ is also independent of δ (see (51) below). This conjecture is the one that should be verified with the help of the data extracted out from ordinary or numerical experiments. We will see this in the present paper. Note that, with the new number $\tilde{n}$, ℓ_n introduced in (1) reduces to $\ell_n = \ell_0 \mathrm{e}^{-\tilde{n}}$, and that $\tilde{n}$ may provide us with a common number of steps appropriate for the interpretation of turbulence within the cascade model.

In this paper, we will investigate in a high accuracy the validity of the new scaling relation (3), which MPDFT claimed as a physically required relation for arbitrary value of δ. This is performed by analyzing the series of PDFs for energy transfer rates extracted by Kaneda and Ishihara from their 4096^3 DNS for fully developed turbulence with the magnification rate $\delta = 2^{1/4}$ [30]. The theoretical PDF formula for physical quantities within MPDFT is provided with the minimal numbers of adjustable parameters, i.e., one parameter for the partial PDF at the tail region and two parameters for the partial PDF at the center region. Note that the theoretical PDF is given by two partial PDFs, one for the tail part and the other for center part. This is realized with the help of the Tsallis-type trial functions. By means of the behavior of extracted parameters, we can check the validity of the new scaling relation, and obtain the information about how to separate the coherent turbulence motion and the fluctuations around the motion.

The organization of the paper is the following. In section 2, we introduce an exponent representing the degree of singularity for observables responsible to intermittent character of turbulence. The singularity originates from the invariance of the N-S equation under a scale transformation. The PDF for the singular exponents is introduced in section 3 in connection with the multifractal spectrum. Other materials necessary for multifractal description, such as the mass exponent, the generalized dimension and so on, are introduced. Section 4 provides an introduction of the framework of MPDFT with the new scaling relation, and the construction of the PDFs within A&A model whose variable range extends both positive and negative regions. We put in this paper a minimal derivation of necessary formulae in a self-contained manner in order to clarify the logic behind the framework of MPDFT. In section 5, we analyze in a high precision the observed PDFs for energy transfer rates by the theoretical PDF within A&A model of MPDFT, and verify the proposed assumption through the analysis. Summary and prospects are devoted in section 6.

2. Scaling Invariance and Singularities

Let us start with the velocity difference (fluctuation) $\delta u_n = |u(\bullet + \ell_n) - u(\bullet)|$ of a component u of the velocity field $\vec{u}$ between two points separated by the distance ℓ_n, defined by (1), which provides us with the measure of diameters of eddies generated at the nth stage. The diameters of eddies being produced one after another become δ^{-1} times smaller at each generation of eddies from bigger ones. Turbulence is not fluctuating randomly but *intermittently*, i.e., in the intermittent rhythms.

The kinetic energy of eddies with the diameter $\ell_n \sim \ell_n + d\ell_n$ per unit mass is defined by $E_n = \int_{k_n}^{k_{n+1}} dk\ E_k = \delta u_n^2/2$, where we put $k_n = \ell_n^{-1}$. The velocity

difference δu_n gives the order of the rotational velocity of the eddy. E_k is called the energy spectrum. There are two characteristic times (relaxation times) for the eddy. One is the time necessary for the eddy to rotate once, i.e., $t_n = \ell_n/\delta u_n$. This can be interpreted as the time (life-time) for the eddy with the diameter ℓ_n to pass its kinetic energy to eddies with the diameter $\ell_{n+1} = \delta^{-1}\ell_n$. Then, the energy transfer rate ϵ_n from the eddies with the diameter ℓ_n to the eddies with ℓ_{n+1} may be estimated as

$$|\epsilon_n| \sim E_n/t_n \sim (\delta u_n)^3/\ell_n. \tag{5}$$

We interpret it as follows; At each step in the cascade, say the nth step, where an eddy breaks up into δ pieces, the energy is delivered from the eddy with the diameter ℓ_n to those with ℓ_{n+1} with the energy transfer rate ϵ_n per unit mass. Another characteristic time is the time required for the energy of eddies to dissipate into heat, i.e., $t_n^{\rm diss} \sim \ell_n^2/\nu$. This is given as a quantity having the dimension of time by making use of the fact that the kinematic viscosity ν has the dimension $[\nu] = \mathrm{L}^2/\mathrm{T}$. The energy dissipation rate ε_n averaged in the regions with diameter ℓ_n is given by [1]

$$\varepsilon_n \sim \nu_n \left(\delta u_n/\ell_n\right)^2 \tag{6}$$

where ν_n is the kinematic viscosity associated with the eddies under consideration. For the condition $t_n \ll t_n^{\rm diss}$, the dissipative effect to eddies can be neglected, whereas for $t_n \gg t_n^{\rm diss}$ no eddy can survive as its rotational energy is transferred into heat almost all at once.

Kolmogorov assumed in 1941 (K41) [31, 32] in his explanation of the universal slope $-5/3$ observed in the energy spectrum of turbulence that, in the region where the condition $t_n \ll t_n^{\rm diss}$ is satisfied and the effect of dissipation is safely neglected, ϵ_n is constant and does not depend on n, i.e., $\epsilon_n = \epsilon$ (> 0). Substituting this into (5), we have $\delta u_n \sim (\epsilon\ell_n)^{1/3}$, $E_n \sim (\epsilon\ell_n)^{2/3}$. Then, we see that $t_n \sim \left(\ell_n^2/\epsilon\right)^{1/3}$, and that the smaller the eddies become, the shorter their life-times become in the delivery of their energy. The lifetime τ_η and the diameter η of the eddy satisfying the condition $t_n = t_n^{\rm diss}(= \tau_\eta)$ are estimated, respectively, as

$$\tau_\eta = \left(\nu/\epsilon\right)^{1/2}, \quad \eta = \left(\nu^3/\epsilon\right)^{1/4}, \tag{7}$$

which are called the Kolmogorov time and the Kolmogorov length, respectively.

The scaling exponent ζ_m of the mth order velocity structure function (the mth moment of velocity fluctuations) defined through

$$\langle (\delta u_n/\delta u_0)^m \rangle = (\ell_n/\ell_0)^{\zeta_m} \tag{8}$$

is one of the quantities which characterizes turbulence. Here, $\langle \cdots \rangle$ indicates to take an appropriate time average, spatial average or ensemble average. Actually, the present main issue is to search for an appropriate PDF for the average. The scaling exponents for K41 [31, 32] are given by $\zeta_m = m/3$.

We consider an incompressible fluid where the mass density $\rho = \rho(\vec{x}, t)$ of the fluid is constant in time and space. In this case, the N-S equation for the velocity

[1] Note that we are using the character ε for the energy dissipation rate, whereas the character ϵ for the energy transfer rate.

field $\vec{u} = \vec{u}(\vec{x}, t)$ reduces to

$$\partial\vec{u}/\partial t + (\vec{u}\cdot\vec{\nabla})\vec{u} = -\vec{\nabla}p + \nu\nabla^2\vec{u} \tag{9}$$

where we introduced $p = \hat{p}/\rho$, and the kinematic viscosity $\nu = \hat{\eta}/\rho$. Here, $\hat{p} = \hat{p}(\vec{x}, t)$ is the pressure of fluid, and $\hat{\eta}$ is the viscosity. The condition for incompressibility reduces to the equation representing that there is no divergence in velocity field, i.e., $\vec{\nabla}\cdot\vec{u} = 0$. The N-S equation (9) is invariant under the scale transformation

$$\vec{x} \to \vec{x}' = \lambda\vec{x}, \quad \vec{u} \to \vec{u}' = \lambda^{\alpha/3}\vec{u}, \quad t \to t' = \lambda^{1-\alpha/3}t, \quad p \to p' = \lambda^{2\alpha/3}p \tag{10}$$

and

$$\nu \to \nu' = \lambda^{1+\alpha/3}\nu \tag{11}$$

with an arbitrary real number α. By the way, in the region where the intermittency of turbulence is conspicuous, the effect of the dissipative term in the N-S equation is very small compared with those of other terms (especially, the drift term). Therefore, let us try to extract the phenomena which is invariant under the scale transformation (10) without (11).[1] We utilize the invariance under this scale transformation in order to introduce at the zero-th order approximation the characteristics that the appearance of the velocity field for fully developed turbulence is invariant even if we change the scale (or the distance) of observation. However, we should keep in mind that the dissipative term can become effective depending on the region under consideration since the term breaking the invariance does exist, i.e., non-zero (see the discussions in the following).

Let us now find out what character the system has when it is invariant under the transformation (10). The scale transformation gives

$$\delta u_n/\delta u_0 = (\ell_n/\ell_0)^{\alpha/3}, \quad \delta p_n/\delta p_0 = (\ell_n/\ell_0)^{2\alpha/3}. \tag{12}$$

The difference $\delta p_n = |p(\bullet + \ell_n) - p(\bullet)|$ is also an important observable. From (5) and (12), we also have

$$|\epsilon_n|/\epsilon = (\ell_n/\ell_0)^{\alpha-1}, \tag{13}$$

where we put $\epsilon_0 = \epsilon$. As for the energy dissipation rate ε_n, we need the scale transformation (11) giving

$$\nu_n/\nu_0 = (\ell_n/\ell_0)^{1+\alpha/3} \tag{14}$$

since the dissipative term is necessary for energy dissipation. Then, (6) gives us

$$\varepsilon_n/\epsilon = (\nu_n/\nu_0)\,(\delta u_n/\delta u_0)^2\,(\ell_0/\ell_n)^2 = (\ell_n/\ell_0)^{\alpha-1} \tag{15}$$

where we put $\varepsilon_0 = \epsilon$. Here, we introduced an interpretation of the energy balance of eddies with diameter ℓ_n in a stationary state such that the input energy with the rate $|\epsilon_{n-1}|$ for the eddies should go out from them with the effective energy

[1]Strictly speaking, the N-S equation (9) is invariant under this transformation only the case $\nu = 0$, i.e., when the Reynolds number is infinite.

dissipation rate ε_n obtained by averaging the actual energy dissipation rates in the region specified by ℓ_n. Note that the actual dissipation rates exist for $\ell_n < \eta$.

The velocity derivative u' and the fluid particle acceleration $\vec{\mathrm{a}}$ are described,[1] respectively, by $|u'| = \lim_{n\to\infty} u'_n$, $|\vec{\mathrm{a}}| = \lim_{n\to\infty} \mathrm{a}_n$. Here, we introduced the *velocity derivative* u'_n and *acceleration* a_n corresponding to the characteristic length ℓ_n by $u'_n = \delta u_n/\ell_n$, $\mathrm{a}_n = \delta p_n/\ell_n$, respectively. We see that the velocity derivative and the fluid particle acceleration, respectively, have singularities [2] for $\alpha < 3$ and $\alpha < 1.5$, i.e., $|u'| \propto \lim_{\ell_n\to 0} \ell_n^{(\alpha/3)-1} \to \infty$, $|\vec{\mathrm{a}}| \propto \lim_{\ell_n\to 0} \ell_n^{(2\alpha/3)-1} \to \infty$. The energy transfer rate and the energy dissipation rate also have singularities for $\alpha < 1$, i.e., $\lim_{n\to\infty} |\epsilon_n| = \lim_{n\to\infty} \varepsilon_n = \lim_{n\to\infty} \ell_n^{\alpha-1} \to \infty$. The exponent α plays the role of an index representing the degree of singularities [2].

Within the treatment of K41 [31, 32], as ϵ_n is assumed to be constant independent of n, we see from (13) that K41 is the case corresponding to $\alpha = 1$. If we look at this way, the arbitrariness of α, appeared in the scale transformation (10), indicates that ϵ_n can be viewed as a stochastic variable, i.e., one can introduce fluctuations in ϵ_n. It means that there is a possibility to give an answer to the criticism against K41 raised by Landau. In other words, the energy transfer rate ϵ_n can take various values even for the eddies with the same diameter.[3] The distribution of the values, i.e., the distribution of α, is determined by a delicate balance between the nonlinear convective term and the dissipative term in the N-S equation.

3. Distribution of α and Multifractal Spectrum

One needs $(\ell_n/\ell_0)^{-d}$ boxes in order to cover whole the space of volume 1^d in d dimensional space by the boxes with volume $(\ell_n/\ell_0)^d$ without vacancy. Let us derive, following the argument given by Meneveau and Sreenivasan [5], the probability $P^{(n)}(\alpha)d\alpha$ to find a value within the domain $\alpha \sim \alpha + d\alpha$ when we pay attention to one of the boxes with volume $(\ell_n/\ell_0)^d$ in d dimensional space. Under the assumption that the eddies specified by α occupy the space with the fractal dimension $f_d(\alpha)$, the probability is given by the proportion of the number $(\ell_n/\ell_0)^{-f_d(\alpha)}$ of boxes, occupying $f_d(\alpha)$ dimensional space without vacancy, to the number $(\ell_n/\ell_0)^{-d}$ of all the boxes, i.e.,

$$P^{(n)}(\alpha)d\alpha = c_2(\alpha)\,(\ell_n/\ell_0)^{d-f_d(\alpha)}\,d\alpha. \tag{16}$$

The fractal dimension $f_d(\alpha)$ is called the multifractal spectrum.

For $\varepsilon_n \neq 0$, (15) shows that α is related with ε_n by $\alpha = 1 + \ln(\varepsilon_n/\epsilon)/\ln(\ell_n/\ell_0)$. Then, the probability $P^{(n)}(\alpha)d\alpha$ is rewritten in terms of the conditional probability $P^{(n)}_{\varepsilon}(\varepsilon_n/\epsilon \mid \varepsilon_n \neq 0)d(\varepsilon_n/\epsilon)$ to find in the box a non-zero value ε_n/ϵ between the domain $\varepsilon_n/\epsilon \sim \varepsilon_n/\epsilon + d(\varepsilon_n/\epsilon)$ as

$$P^{(n)}(\alpha)d\alpha = P^{(n)}_{\epsilon}\,(\varepsilon_n/\epsilon \mid \varepsilon_n \neq 0)\,d\,(\varepsilon_n/\epsilon)\,P^{(n)}_{\varepsilon_n\neq 0}. \tag{17}$$

Here, $P^{(n)}_{\varepsilon_n\neq 0}$ is the probability that the selected box satisfies the condition $\varepsilon_n \neq 0$. Assuming that the boxes satisfying $\varepsilon_n \neq 0$ occupy D_d dimensional space without

[1]The fluid particle acceleration $\vec{\mathrm{a}}$ is given by $\vec{\mathrm{a}} = \partial\vec{u}/\partial t + (\vec{u}\cdot\vec{\nabla})\vec{u}$.

[2]In practice, as the resolutions in experiments or numerical simulations are finite, it may be appropriate to interpret that the term *singularity* here means to take abnormally large values.

[3]From (12), we interpret that the velocity fluctuation and the pressure fluctuation are also stochastic variables.

vacancy, we can estimate $P^{(n)}_{\varepsilon_n\neq 0}$ as the proportion of the number $(\ell_n/\ell_0)^{-D_d}$ of boxes satisfying $\varepsilon_n \neq 0$ to the number $(\ell_n/\ell_0)^{-d}$ of all the boxes, i.e.,

$$P^{(n)}_{\varepsilon_n\neq 0} = c_1 \left(\ell_n/\ell_0\right)^{d-D_d}. \tag{18}$$

Substituting (18) and (16) into (17), one obtains [5]

$$P^{(n)}_{\epsilon}\left(\varepsilon_n/\epsilon\right) = \left[c_2(\alpha)/c_1 \ln\left(\ell_n/\ell_0\right)\right] \ \left(\ell_n/\ell_0\right)^{1+D_d-\alpha-f_d(\alpha)}. \tag{19}$$

In the following, we will proceed the investigation assuming that the α dependence of the normalization coefficient $c_2(\alpha)$ is negligible.

The mass exponent $\tau_d(\bar{q})$ is introduced by means of the partition function [5]

$$Z^{(n)}_d \equiv \sum_{\#\text{ of boxes}} \left(\varepsilon_n \ell_n^d/\epsilon\ell_0^d\right)^{\bar{q}} = \sum_{\#\text{ of boxes}} \left(\ell_n/\ell_0\right)^{(\alpha-1+d)\bar{q}} \propto \left(\ell_n/\ell_0\right)^{-\tau_d(\bar{q})}. \tag{20}$$

The summation with respect to the number of boxes may be translated into the integration with respect to α as

$$Z^{(n)}_d = \int d\alpha\rho(\alpha) \ \left(\ell_n/\ell_0\right)^{(\alpha-1+d)\bar{q}-f_d(\alpha)}. \tag{21}$$

Evaluating the integration with the help of the method of the steepest descent in the limit $\ell_n/\ell_0 \to 0$, i.e., $n\to\infty$, we obtain the relation [1]

$$f_d(\alpha) - (\alpha - 1 + d)\bar{q} = \tau_d(\bar{q}), \quad \bar{q} = df_d(\alpha)/d\alpha. \tag{22}$$

With

$$\alpha - 1 + d = -d\tau_d(\bar{q})/d\bar{q}, \tag{23}$$

(22) constitutes the Legendre transformation between $f_d(\alpha)$ and $\tau_d(\bar{q})$. The generalized dimension (the Rényi dimension) $D_d(\bar{q})$ is introduced by the relation

$$\tau_d(\bar{q}) = (1-\bar{q})D_d(\bar{q}). \tag{24}$$

The $\bar{q}$th moment of the energy transfer rate is given by using the mass exponent as

$$\left\langle (\varepsilon_n/\epsilon)^{\bar{q}} \right\rangle \equiv \int_0^\infty d\left(\varepsilon_n/\epsilon\right) \ \left(\varepsilon_n/\epsilon\right)^{\bar{q}} P^{(n)}_{\epsilon}\left(\varepsilon_n/\epsilon\right) \sim \left(\ell_n/\ell_0\right)^{-\tau_d(\bar{q})+D_d-\bar{q}d}. \tag{25}$$

The condition for the normalization of probability, i.e., $\langle 1\rangle = 1$, reduces to

$$\tau_d(0) = D_d = D_d(\bar{q}=0) = f_d(\alpha_{\bar{q}=0}). \tag{26}$$

Whereas, the energy conservation law, i.e., $\langle \varepsilon_n\rangle = \epsilon$, reduces to

$$\tau_d(1) = D_d - d. \tag{27}$$

[1] We are neglecting the α dependence of the density $\rho(\alpha)$ introduced in the translation $\sum_{\#\text{ of boxes}} = \int d\alpha\rho(\alpha) \ \left(\ell_n/\ell_0\right)^{-f_d(\alpha)}$.

Since $\tau_d(1) = 0$ in general when $D_d(1)$ is finite, (27) gives

$$D_d = D_d(\bar{q} = 0) = d. \tag{28}$$

The definition of the intermittency exponent μ, i.e., $\left\langle \varepsilon_n^2 \right\rangle = \epsilon^2 \left(\ell_n/\ell_0\right)^{-\mu}$, provides us with

$$\mu = \tau_d(2) - D_d + 2d. \tag{29}$$

Summarizing (26), (28) and (29), we have

$$\tau_d(0) = D_d(\bar{q} = 0) = d, \quad \tau_d(1) = 0, \quad \mu = d + \tau_d(2) = d - D_d(2). \tag{30}$$

Note that the first equation in (30) is also obtained by noticing that the number of boxes with the side length ℓ_n necessary to cover the d dimensional space is given by $\sum_{\#\text{ of boxes}} 1 \propto \left(\ell_n/\ell_0\right)^{-d}$, and that $\sum_{\#\text{ of boxes}} 1 \propto \left(\ell_n/\ell_0\right)^{-\tau_d(0)}$ from (20), i.e., the definition of $\tau_d(\bar{q})$. Notice that the scaling exponent of the mth order velocity structure function defined by (8) is related to the mass exponent as

$$\zeta_m = d - \tau_d\left(m/3\right) + (1-d)m/3. \tag{31}$$

It is convenient to introduce $f(\alpha)$ and $\tau(\bar{q})$, respectively, through the relations

$$f_d(\alpha) = f(\alpha) + d - 1, \quad \tau_d(\bar{q}) = \tau(\bar{q}) + (d-1)(1-\bar{q}), \tag{32}$$

and $D(\bar{q})$ by

$$\tau(\bar{q}) = (1-\bar{q})D(\bar{q}). \tag{33}$$

Note that $D_d(\bar{q})$ and $D(\bar{q})$ are related with each other by

$$D_d(\bar{q}) = D(\bar{q}) + d - 1. \tag{34}$$

Then, the Legendre transformation, consisting of (22) and (23), reduces to

$$f(\alpha) = \alpha\bar{q} + \tau(\bar{q}), \quad \bar{q} = df(\alpha)/d\alpha, \quad \alpha = -d\tau(\bar{q})/d\bar{q}, \tag{35}$$

and the relations in (30) and the one in (31), respectively, to

$$\tau(0) = D(0) = f(\alpha_0) = 1, \quad \tau(1) = 0, \quad \mu = 1 + \tau(2) = 1 - D(2) \tag{36}$$

and

$$\zeta_m = 1 - \tau\left(m/3\right). \tag{37}$$

The probability (16) reduces to

$$P^{(n)}(\alpha)d\alpha \propto \left(\ell_n/\ell_0\right)^{1-f(\alpha)} d\alpha \tag{38}$$

by making use of the first equation in (32). It is worthwhile to note that the system with $f(\alpha)$, $\tau(\bar{q})$ and $D(\bar{q})$ is not only for the analyses of multifractal structure of data-set with $d = 1$ but also for those with general dimension $d > 1$. The

(multi)-fractal structures in d-dim are accumulated altogether into the (multi)-fractal dimension $f(\alpha) = f_d(\alpha) - (d-1)$.

It is the log-normal model [22–24] that was proposed to take in the intermittency of turbulence by introducing fluctuation of ε_n, in the form of the first reply to the criticism raised by Landau. The ratios $\varepsilon_n/\varepsilon_{n-1}$ $(n = 1, 2, \cdots)$ of the energy dissipation rates, which is interpreted as a measure how much energy received by the eddy with the diameter ℓ_{n-1} is delivered to the eddy of the size ℓ_n, are regarded as stochastic variables defined within the domain $[0, \infty]$. Let us assume that the variables specified by n are, mutually, stochastically independent, and that they have an identical distribution function. In this case, the distribution of the stochastic variable

$$\left(1/\sqrt{n\sigma^2}\right) \sum_{j=1}^{n} \ln\left(\varepsilon_j/\varepsilon_{j-1}\right) = \left(\sqrt{n}/\sigma\right)(1-\alpha)\ln\delta \tag{39}$$

must be the canonical distribution (Gaussian distribution)

$$P^{(n)}(\alpha) \propto \mathrm{e}^{-n(\alpha-\alpha_0)^2/2\sigma^2} \tag{40}$$

because of the central limit theorem for $n \gg 1$. The domain of α is $[-\infty, \infty]$. The two parameters α_0 and σ are determined as the functions of μ in the forms

$$\alpha_0 = 1 + \mu/2, \quad \sigma^2 = \mu/\ln\delta, \tag{41}$$

respectively, with the help of the two independent relations, i.e., the energy conservation law given by the second equation in (36) and the definition of the intermittency exponent μ given by the third equation in (36). Substituting (41) into (40), we have

$$P^{(n)}(\alpha) \propto \mathrm{e}^{-\tilde{n}(\alpha-1-\mu/2)^2/2\mu} \tag{42}$$

with (4), which does not depend on the magnification δ. Substituting (40) into the left-hand side of (38), we have with (41)

$$f(\alpha) = 1 - (\alpha-\alpha_0)^2/2\sigma^2\ln\delta = 1 - (\alpha-1-\mu/2)^2/2\mu \tag{43}$$

whose final expression is not dependent on δ nor on $\tilde{n}$. Then the mass exponent becomes

$$\tau(\bar{q}) = (1-\bar{q})(1-\mu\bar{q}/2) \tag{44}$$

through the Legendre transformation (22). Therefore, the generalized dimension for the log-normal model becomes $D(\bar{q}) = 1 - \mu\bar{q}/2$.

Note that μ should not depend on δ since μ is unique once a turbulent system is specified, and that the dependence of $P^{(n)}(\alpha)$ on δ is absorbed into σ^2 with the help of $\tilde{n}$. It may be reasonable to interpret $\tilde{n}$ as the "renormalized" number of stages in the cascade model.

4. Theoretical Framework of MPDFT

4.1. *A&A Model*

A&A model within MPDFT [10–13, 15, 16, 18, 19, 21] adopts for $P^{(n)}(\alpha)$ the Tsallis-type distribution function [1]

$$P^{(n)}(\alpha) \propto \left[1-(\alpha-\alpha_0)^2/(\Delta\alpha)^2\right]^{n/(1-q)} \tag{45}$$

with

$$\Delta\alpha = \sqrt{2X/(1-q)\ln\delta} \tag{46}$$

and the entropy index q. The domain of α is $\alpha_{\min} \le \alpha \le \alpha_{\max}$ where $\alpha_{\min}$ and $\alpha_{\max}$ are given by $\alpha_{\min,\,\max} = \alpha_0 \mp \Delta\alpha$. The proportional coefficient in (45) is specified by the normalization condition

$$\int_{\alpha_{\min}}^{\alpha_{\max}} d\alpha\; P^{(n)}(\alpha) = 1. \tag{47}$$

Substituting (45) into the left-hand side of (38), we obtain, for $n \gg 1$, the multifractal spectrum

$$f(\alpha) = 1 + \left\{\ln\left[1-(\alpha-\alpha_0)^2/(\Delta\alpha)^2\right]\right\}/(1-q)\ln\delta \tag{48}$$

whose Legendre transformation provides us with the mass exponent in the form

$$\tau(\bar{q}) = 1-\alpha_0\bar{q}+2X\bar{q}^2\Big/\left(1+\sqrt{C_{\bar{q}}}\right)+\left[1-\log_2\left(1+\sqrt{C_{\bar{q}}}\right)\right](\ln 2)/(1-q)\ln\delta \tag{49}$$

with $C_{\bar{q}} = 1+2\bar{q}^2(1-q)X\ln\delta$. For large $|\bar{q}|$, there appears in $\tau(\bar{q})$ the log term, $\log_2|\bar{q}|$, which is the one of the characteristics of A&A model.

The three parameters α_0, X and q are determined as the functions of μ with the help of the three conditions, i.e., the energy conservation law given by the second equation in (36), the definition of the intermittency exponent given by the third equation in (36), and the scaling relation (3) with $\alpha_\pm = \alpha_0 \pm \sqrt{2bX}$ where $b = \left(1-\mathrm{e}^{-(1-q)\ln\delta}\right)/(1-q)\ln\delta$. As was indicated below (3), $\alpha_\pm$ are the solutions of $f(\alpha_\pm) = 0$, i.e., $f_d(\alpha_\pm) = d-1$. Here, the multifractal spectrum $f(\alpha)$ is given by (48). The scaling relation (3) is a generalization of the one introduced by Tsallis and others [25, 26] to which (3) reduces, when $\delta = 2$. This generalization was born out of the theoretical framework, A&A model within MPDFT, itself. The new scaling relation (3) is solved as

$$\sqrt{2bX} = -(1-q)\log_2\delta + \sqrt{\alpha_0^2 + \left[(1-q)\log_2\delta\right]^2}, \tag{50}$$

and the parameter q is determined, altogether with α_0 and X, as a function of μ only in the combination $(1-q)\ln\delta$. It is quite reasonable in the following reason. The value of the magnification δ is determined arbitrarily by observers, therefore its value should not affect the values of physical quantities as long as one studies a

[1] Regardless if the fundamental entropy is the extensive Rényi entropy or the non-extensive HCT entropy, the MaxEnt PDFs which give the extremum of these entropies have a common structure. Within the present approach, one cannot determine which is the background entropy for turbulence.

turbulent system. The difference in δ is absorbed into the entropy index q, which may be reasonable in the sense that changing the zooming rate δ may result in picking up the different hierarchy, containing the entropy specified by the index q, out of multifractal structure of turbulence. The detailed investigation of this point will be given elsewhere.

With the above generalization of the scaling relation, as the parameters are dependent on q only in the combination $(1-q)\ln\delta$, we are naturally lead to the replacement of n in the expression of $P^{(n)}(\alpha)$ in (45) with $\tilde{n}$ defined by (4), i.e.,

$$P^{(n)}(\alpha) \propto \left[1-(\alpha-\alpha_0)^2/(\Delta\alpha)^2\right]^{\tilde{n}/(1-q)\ln\delta}. \tag{51}$$

If it is revealed that $\tilde{n}$ does not depend on δ, the distribution of α itself becomes also independent of δ. Then, A&A model within MPDFT has come to the framework in which the choice of the magnification δ does not affect the PDF for α in addition to observables. Note that the new scaling relation (3) is found to be intimately related to δ-scale Cantor sets produced by a series of the unstable δ^∞ periodic orbits. $\tilde{n}$ may be interpreted as the number of *stages* in the δ-scale Cantor set, and can be understood, intuitively, as the number of stages in the energy cascade model.

4.2. *PDFs for Observables*

Now, we derive the general formula for PDFs within MPDFT for an observable

$$|x'| = \lim_{n\to\infty}|x'_n|, \quad |x'_n| = (\delta x_n/\ell_n)\,/\,(\delta x_0/\ell_0) \tag{52}$$

representing intermittent singular behavior, where $\delta x_n = |x(\bullet+\ell_n) - x(\bullet)|$ is the fluctuation of a physical quantity x, and is assumed to be related to α through

$$|x_n| = \delta x_n/\delta x_0 = (\ell_n/\ell_0)^{\phi\alpha/3}. \tag{53}$$

Since

$$|x'_n| = |x_n|\,(\ell_n/\ell_0)^{-1} = (\ell_n/\ell_0)^{(\phi\alpha/3)-1}, \tag{54}$$

$|x'|$ diverges for $\alpha < 3/\phi$. Note that $|x'|$ reduces to the velocity derivative and fluid particle acceleration for $\phi = 1$ and $\phi = 2$, respectively, and formally to the energy transfer rates (13) or the energy dissipation rates (15) for $\phi = 3$. The probability $\Pi'^{(n)}_\phi(x'_n)dx'_n$ to find the physical quantity x'_n taking a value in the domain $x'_n \sim x'_n + dx'_n$ is supposed to be rephrased by the probability $\Pi^{(n)}_\phi(x_n)dx_n$ to find the physical quantity x_n taking a value in the domain $x_n \sim x_n + dx_n$ with the relation

$$\Pi'^{(n)}_\phi(x'_n)dx'_n = \Pi^{(n)}_\phi(x_n)dx_n. \tag{55}$$

Let us assume that the PDF $\Pi^{(n)}_\phi(x_n)$ can be divided into two parts as

$$\Pi^{(n)}_\phi(x_n) = \Pi^{(n)}_{\phi,\mathrm{S}}(x_n) + \Delta\Pi^{(n)}_\phi(x_n). \tag{56}$$

Here, the first term describes the contribution from the abnormal part of the physical quantity x_n due to the fact that its singularities distribute themselves multi-

fractal way in real space. It is the part given by

$$\Pi^{(n)}_{\phi,\mathrm{S}}(|x_n|)d|x_n| = \bar{\Pi}^{(n)}_{\phi,\mathrm{S}}\ P^{(n)}(\alpha)d\alpha \tag{57}$$

through the variable translation (53) between $|x_n|$ and α. On the other hand, the second term $\Delta\Pi^{(n)}_{\phi}(x_n)$ represents the contributions from the dissipative term in the N-S equation and/or from the errors in measurements, etc.. The dissipative term violates the invariance based on the scale transformation (10), and, therefore, the effect of dissipation has been neglected in the consideration of $\Pi^{(n)}_{\phi,\mathrm{S}}(x_n)$ for the distribution of singularities. The second term in (56) is a correction to the first one in the analysis of observed PDF. The values of $|x_n|$ representing the part originated from the singularities are describing the part larger than the standard deviation due to intermittency. The values of $|x_n|$ for the part contributing to the correction term are smaller than or about the order of its standard deviation.

4.3. *PDFs for Variables taking Positive and Negative Values*

Let us consider the PDF for the variable x'_n whose range is $(-\Lambda_n,\ \Lambda_n)$. The mth moment of $|x'_n|$ is translated into the mth moment of the structure functions for the variable $|x_n|$, i.e.,

$$\int_{-\Lambda_n}^{\Lambda_n} dx'_n|x'_n|^m\Pi'^{(n)}_{\phi}(x'_n) = (\ell_n/\ell_0)^{-m}\,\langle\langle|x_n|^m\rangle\rangle \tag{58}$$

where

$$\langle\langle|x_n|^m\rangle\rangle = \int_{-\Lambda_n}^{\Lambda_n} dx_n|x_n|^m\Pi^{(n)}_{\phi}(x_n) \tag{59}$$

with

$$\Lambda_n = (\ell_n/\ell_0)^{(\phi\alpha_{\min}/3)-1}\,. \tag{60}$$

The normalization of $\Pi'^{(n)}_{\phi}(x'_n)$ is given by

$$\int_{-\Lambda_n}^{\Lambda_n} dx'_n\Pi'^{(n)}_{\phi}(x'_n) = \langle\langle 1\rangle\rangle = 1. \tag{61}$$

Substituting (56) with (57) into (59), we have

$$\begin{aligned}\langle\langle|x_n|^m\rangle\rangle &= 2\int_0^{\Lambda_n} dx_n\ (x_n)^m\Pi^{(n)}_{\phi,\mathrm{S}}(x_n) + 2\gamma^{(n)}_{\phi,m}\\ &= 2\bar{\Pi}^{(n)}_{\phi,\mathrm{S}}\int_{\alpha_{\min}}^{\alpha_{\max}} d\alpha\ \ (\ell_n/\ell_0)^{\phi m\alpha/3}\,P^{(n)}(\alpha) + 2\gamma^{(n)}_{\phi,m}\\ &= 2\bar{\Pi}^{(n)}_{\phi,\mathrm{S}}\ a_{\phi m}\ \ (\ell_n/\ell_0)^{1-\tau(\phi m/3)} + 2\gamma^{(n)}_{\phi,m}\end{aligned} \tag{62}$$

with

$$\gamma^{(n)}_{\phi,m} = \int_0^{\Lambda_n} dx_n\,(x_n)^m\,\Delta\Pi^{(n)}_{\phi}(x_n), \tag{63}$$

$$a_{\phi m} = \sqrt{|f''(\alpha_0)|/|f''(\alpha_{\phi m/3})|} \tag{64}$$

where $f''(\alpha) = d^2 f(\alpha)/d\alpha^2$. The third equality in (62) is estimated for $n \gg 1$. For $m = 0$, (62) gives $\langle\langle 1 \rangle\rangle = 1$ with the normalization condition (61), hence we have

$$\bar{\Pi}^{(n)}_{\phi,\mathrm{S}} = \left(1 - 2\gamma^{(n)}_{\phi,0}\right)/2. \tag{65}$$

Here, we used the facts $a_0 = 1$ and $\tau(0) = 1$. We finally obtain the compact expression for the mth moment of the structure function in the form

$$\langle\langle |x_n|^m \rangle\rangle = 2\gamma^{(n)}_{\phi,m} + (1 - 2\gamma^{(n)}_{\phi,0})\ a_{\phi m}\ \ (\ell_n/\ell_0)^{\zeta_{\phi m}} \tag{66}$$

with the corresponding scaling exponents

$$\zeta_{\phi m} = 1 - \tau\left(\phi m/3\right). \tag{67}$$

For $\phi = 1$, $\zeta_{\phi m}$ reduces to the scaling exponents ζ_m of the mth order velocity structure function defined by (8). Note that $\Pi^{(n)}_{\phi,\mathrm{S}}(x_n)dx_n$ now has the compact form

$$\Pi^{(n)}_{\phi,\mathrm{S}}(|x_n|)d|x_n| = \frac{1 - 2\gamma^{(n)}_{\phi,0}}{2}\sqrt{\frac{|f''(\alpha_0)||\ln\left(\ell_n/\ell_0\right)|}{2\pi}}\ \left(\frac{\ell_n}{\ell_0}\right)^{1-f(\alpha)} d\alpha. \tag{68}$$

It is convenient to introduce the PDF

$$\hat{\Pi}^{(n)}_{\phi}(\xi_n)\ d\xi_n = \Pi^{(n)}_{\phi}(x'_n)\ dx'_n \tag{69}$$

for the variable

$$\xi_n = x'_n/\sqrt{\langle\langle (x'_n)^2 \rangle\rangle} = x_n/\sqrt{\langle\langle (x_n)^2 \rangle\rangle} \tag{70}$$

normalized by the standard deviation. The normalized variable ξ_n is related to α through the relation

$$|\xi_n| = \bar{\xi}_n\left(\ell_n/\ell_0\right)^{(\phi\alpha/3)-\zeta_{2\phi}/2} \tag{71}$$

with

$$\bar{\xi}_n = \left[2\gamma^{(n)}_{\phi,2}\left(\ell_n/\ell_0\right)^{-\zeta_{2\phi}} + \left(1 - 2\gamma^{(n)}_{\phi,0}\right)a_{2\phi}\right]^{-1/2}. \tag{72}$$

It is reasonable to assume that the origin of intermittent rare events is attributed to the first singular term in (56), and that the contribution from the second term $\Delta\Pi^{(n)}_{\phi}(x_n)$ to the events is negligible. Therefore, we put, for $\xi^*_n \le |\xi_n| \le \xi^{\max}_n$ (equivalently, $\alpha_{\min} \le \alpha \le \alpha^*$),

$$\hat{\Pi}^{(n)}_{\phi,\mathrm{tl}}(|\xi_n|)\ d|\xi_n| = \Pi^{(n)}_{\phi,\mathrm{S}}(|x_n|)\ d|x_n|, \tag{73}$$

where

$$\xi^{\max}_n = \bar{\xi}_n\left(\ell_n/\ell_0\right)^{(\phi\alpha_{\min}/3)-\zeta_{2\phi}/2}. \tag{74}$$

Substituting (57) with (38) into (73), we have

$$\hat{\Pi}^{(n)}_{\phi,\mathrm{tl}}(|\xi_n|) = \bar{\Pi}^{(n)}_{\phi}\ (\ell_n/\ell_0)^{(\zeta_{2\phi}/2)-(\phi\alpha/3)+1-f(\alpha)} = \bar{\Pi}^{(n)}_{\phi}\ (\ell_n/\ell_0)^{1-f(\alpha)}\,\bar{\xi}_n/|\xi_n| \quad (75)$$

with

$$\bar{\Pi}^{(n)}_{\phi} = \left[3\left(1-2\gamma^{(n)}_{\phi,0}\right)/2\phi\bar{\xi}_n\right]\sqrt{|f''(\alpha_0)|/2\pi|\ln\left(\ell_n/\ell_0\right)|}. \quad (76)$$

Note that $\xi^*_n \lesssim 1$ as can be seen below when we analyze experiments. This *tail part* $\hat{\Pi}^{(n)}_{\phi,\mathrm{tl}}(|\xi_n|)$ represents the large deviations, and manifests itself the multifractal distribution of the singularities due to the scale invariance of the Navier-Stokes equation when its dissipative term can be neglected.

For smaller values, $|\xi_n| \le \xi^*_n$ (equivalently, $\alpha^* \le \alpha$), we put

$$\hat{\Pi}^{(n)}_{\phi,\mathrm{cr}}(\xi_n)d\xi_n = \left[\Pi^{(n)}_{\phi,\mathrm{S}}(x_n) + \Delta\Pi^{(n)}_{\phi}(x_n)\right]dx_n = \bar{\Pi}^{(n)}_{\phi,\mathrm{cr}}\ \mathrm{e}^{-g_\phi(\xi_n)}d\xi_n \quad (77)$$

with some real valued function $g_\phi(\xi_n)$. The contribution to this *center part* $\hat{\Pi}^{(n)}_{\phi,\mathrm{cr}}(\xi_n)$ comes from a specific fluctuations of the variable smaller than its standard deviation. This part may represent a specific fluctuation which is a mixture of the coherent turbulent motion and the incoherent motion stemmed from the dissipative term violating the scale invariance.

The two parts of the PDF, $\hat{\Pi}^{(n)}_{\phi,\mathrm{tl}}(|\xi_n|)$ and $\hat{\Pi}^{(n)}_{\phi,\mathrm{cr}}(|\xi_n|)$, are connected at

$$\xi^*_n = \bar{\xi}_n\,(\ell_n/\ell_0)^{(\phi\alpha^*/3)-\zeta_{2\phi}/2} \quad (78)$$

under the conditions that they have the common value, i.e.,

$$\hat{\Pi}^{(n)}_{\phi,\mathrm{tl}}(|\xi^*_n|) = \hat{\Pi}^{(n)}_{\phi,\mathrm{cr}}(|\xi^*_n|) \quad (79)$$

and the common log-slope, i.e.,

$$\frac{d}{d\xi_n}\ln\hat{\Pi}^{(n)}_{\phi,\mathrm{tl}}(\xi_n)\Big|_{\xi_n=\xi^*_n} = \frac{d}{d\xi_n}\ln\hat{\Pi}^{(n)}_{\phi,\mathrm{cr}}(\xi_n)\Big|_{\xi_n=\xi^*_n}. \quad (80)$$

The conditions (79) and (80) give

$$\bar{\Pi}^{(n)}_{\phi,\mathrm{cr}} = \bar{\Pi}^{(n)}_{\phi}\ \mathrm{e}^{g_\phi(\xi^\star_n)}\ (\ell_n/\ell_0)^{1-f(\alpha^\star)}\ \bar{\xi}_n/\xi^*_n \quad (81)$$

and

$$dg_\phi(\xi_n)/d\xi_n\big|_{\xi_n=\xi^*_n} = \left[\phi + 3f'(\alpha^*)\right]/\phi\xi^*_n, \quad (82)$$

respectively. With the help of (81), we obtain

$$\hat{\Pi}^{(n)}_{\phi,\mathrm{cr}}(\xi_n) = \bar{\Pi}^{(n)}_{\phi}\mathrm{e}^{-[g_\phi(\xi_n)-g_\phi(\xi^*_n)]}\ (\ell_n/\ell_0)^{1-f(\alpha^\star)}\ \bar{\xi}_n/\xi^*_n. \quad (83)$$

The value of α^*, therefore the value of ξ^*_n (see (78)), is determined for each PDF as an adjusting parameter in the analysis of PDFs obtained by ordinary or numerical

experiments.[1] By this refinement, the PDF $\hat{\Pi}_\phi^{(n)}(\xi_n)$ has come to be able to reproduce experimental PDFs around the connection point much better than before with only negligible changes at the tail part and the center part of the PDF. Note that the reproduction of the PDF for the tail and central parts within MPDFT have been quite satisfactory from the beginning.

With the assumption (73) that, for $\xi_n^* \le |\xi_n| \le \xi_n^{\max}$, one can neglect the contribution from $\Delta\Pi_\phi^{(n)}(x_n)dx_n$, we are able to write down the formula to calculate $2\gamma_{\phi,m}^{(n)}$. From (77), (83) and (68), $\Delta\Pi_\phi^{(n)}(x_n)dx_n$ has its value

$$\Delta\Pi_\phi^{(n)}(x_n)dx_n = \bar{\Pi}_\phi^{(n)} \mathrm{e}^{-[g_\phi(\xi_n)-g_\phi(\xi_n^*)]} \left(\frac{\ell_n}{\ell_0}\right)^{1-f(\alpha^\star)} \frac{\bar{\xi}_n}{\xi_n^*}\, d\xi_n - \frac{1-2\gamma_{\phi,0}^{(n)}}{2}\sqrt{\frac{|f''(\alpha_0)||\ln(\ell_n/\ell_0)|}{2\pi}} \left(\frac{\ell_n}{\ell_0}\right)^{1-f(\alpha)} d\alpha \tag{84}$$

only for the center part, hence, from (63), we have

$$2\gamma_{\phi,m}^{(n)} = 2\int_0^{x_n^*} dx_n (x_n)^m\ \Delta\Pi_\phi^{(n)}(x_n) = \left(1-2\gamma_{\phi,0}^{(n)}\right)\left(K_{\phi,m}^{(n)} - L_{\phi,m}^{(n)}\right) \tag{85}$$

with

$$K_{\phi,m}^{(n)} = \frac{3}{\phi}\left(\frac{\ell_n}{\ell_0}\right)^{1-f(\alpha^*)+m\phi\alpha^*/3} \sqrt{\frac{|f''(\alpha_0)|}{2\pi|\ln(\ell_n/\ell_0)|}} \int_0^1 dz\ z^m \mathrm{e}^{-[g_\phi(\xi_n^* z)-g_\phi(1)]}, \tag{86}$$

$$L_{\phi,m}^{(n)} = \left(\frac{\ell_n}{\ell_0}\right)\sqrt{\frac{|f''(\alpha_0)||\ln(\ell_n/\ell_0)|}{2\pi}} \int_{\alpha^*}^{\alpha_{\max}} d\alpha\ \left(\frac{\ell_n}{\ell_0}\right)^{m\alpha\phi/3-f(\alpha)}. \tag{87}$$

For $m=0$, (85) gives

$$1-2\gamma_{\phi,0}^{(n)} = 1\Big/\left(1+K_{\phi,0}^{(n)} - L_{\phi,0}^{(n)}\right). \tag{88}$$

Then, we finally obtain

$$2\gamma_{\phi,m}^{(n)} = \left(K_{\phi,m}^{(n)} - L_{\phi,m}^{(n)}\right)\Big/\left(1+K_{\phi,0}^{(n)} - L_{\phi,0}^{(n)}\right). \tag{89}$$

The flatness $F_x^{(n)}$ of the PDF for the variable x_n, and therefore of the PDF for x_n', defined by

$$F_x^{(n)} = \langle\langle |x_n|^4\rangle\rangle \big/ \langle\langle |x_n|^2\rangle\rangle^2 = \langle\langle \xi_n^4\rangle\rangle, \tag{90}$$

reduces to

$$F_x^{(n)} = \frac{2\gamma_{\phi,4}^{(n)} + \left(1-2\gamma_{\phi,0}^{(n)}\right) a_{4\phi}\ (\ell_n/\ell_0)^{\zeta_{4\phi}}}{\left[2\gamma_{\phi,2}^{(n)} + \left(1-2\gamma_{\phi,0}^{(n)}\right) a_{2\phi}\ (\ell_n/\ell_0)^{\zeta_{2\phi}}\right]^2}. \tag{91}$$

[1] In the previous treatments, the connection point ξ_n^* had been determined as the point where $\hat{\Pi}_\phi^{(n)}(\xi_n^*)$ has the least dependence on n.

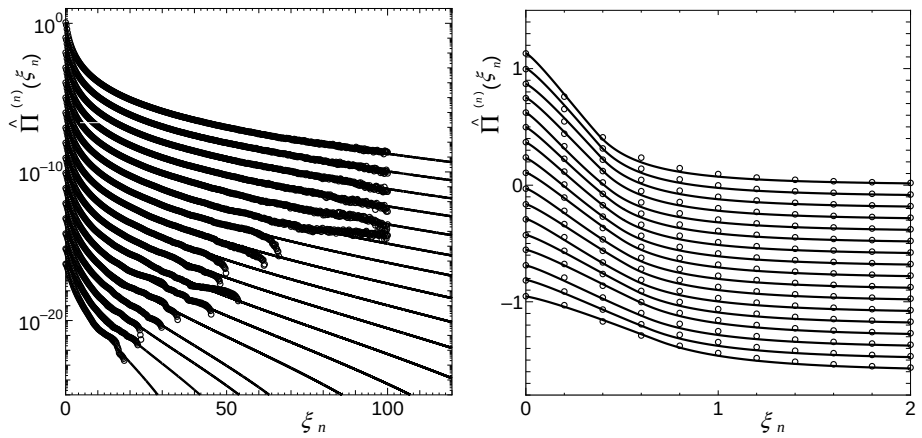

(a) (b)

Figure 1. The PDFs of energy transfer rates for $\delta = 2^{1/4}$ on (a) log and (b) linear scale in the vertical axes. For better visibility, each PDF is shifted by -1 unit along the vertical axis in (a) and by -0.1 unit along the vertical axis in (b). Open circles are the PDFs by DNS from the smallest value (top) to the largest value (bottom) in $2r/\eta$ which are listed in Table 1 where $2r$ corresponds to ℓ_n. Solid lines represent the curves given by the present theory with $\mu = 0.320$ ($(1-q)\ln\delta = 0.323$, $\alpha_0 = 1.19$, $X = 0.382$). Note that $q = -0.862$.

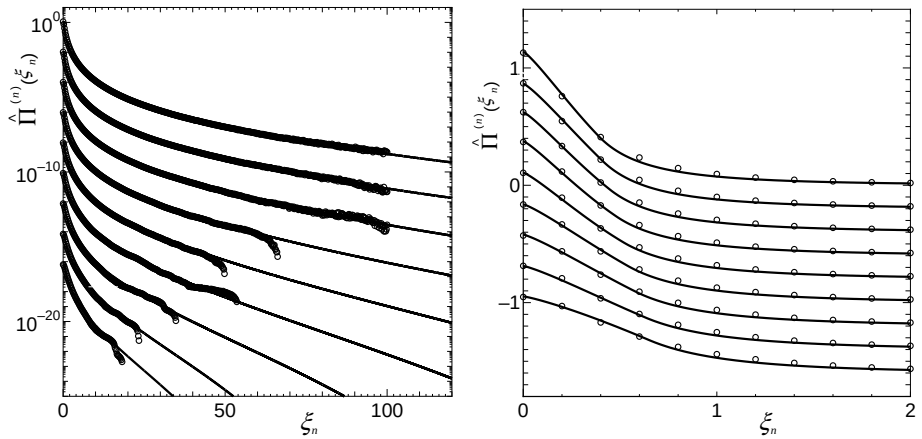

(a) (b)

Figure 2. The PDFs of energy transfer rates for $\delta = 2^{1/2}$ on (a) log and (b) linear scale in the vertical axes. For better visibility, each PDF is shifted by -2 unit along the vertical axis in (a) and by -0.2 unit along the vertical axis in (b). Open circles are the DNS data points for $2r/\eta$ corresponding to the series A for the case $\delta = 2^{1/2}$ in Table 1 where $2r$ corresponds to ℓ_n. Solid lines represent the curves given by the present theory with $\mu = 0.320$ ($(1-q)\ln\delta = 0.323$, $\alpha_0 = 1.19$, $X = 0.382$). Note that $q = 0.068$.

5. Analyses of Observed PDFs for Energy Transfer Rates

In order to see that the value δ actually does not affect the values of observables within the framework of MPDFT, we will analyze the PDFs of energy transfer rates extracted by Kaneda's group from their 4096^3 DNS [30]. The PDFs are symmetrized under the assumption that the intermittent character of turbulence is not affected by the existence of a stationary energy flow which is providing the skewness of the observed PDF for energy transfer rates, since the character originates

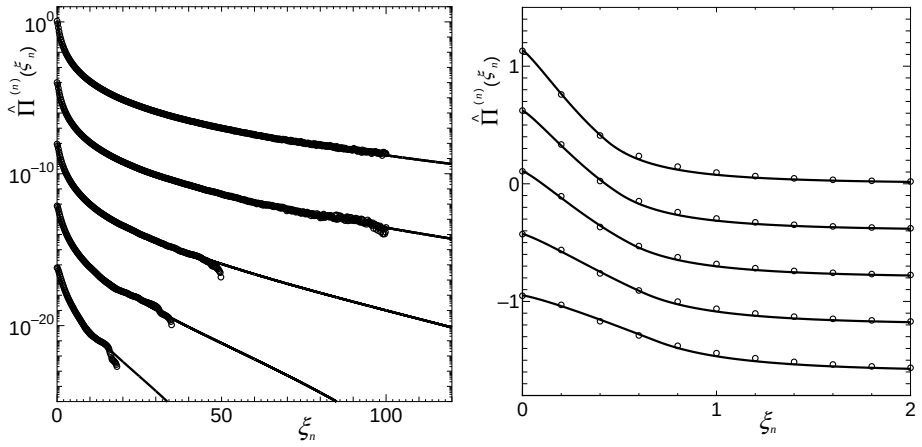

(a) (b)

Figure 3. The PDFs of energy transfer rates for $\delta = 2$ on (a) log and (b) linear scale in the vertical axes. For better visibility, each PDF is shifted by -4 unit along the vertical axis in (a) and by -0.4 unit along the vertical axis in (b). Open circles are the DNS data points for $2r/\eta$ corresponding to the series A for the case $\delta = 2$ in Table 1 where $2r$ corresponds to ℓ_n. Solid lines represent the curves given by the present theory with $\mu = 0.320$ ($(1-q)\ln\delta = 0.323$, $\alpha_0 = 1.19$, $X = 0.382$). Note that $q = 0.534$.

from the multifractal distribution of singularities owing to the invariance of the N-S equation under the scale transformation (10). We believe that the correctness of this assumption is proven by the success in precise re-creation of the symmetrized PDFs by the theoretical PDFs produced under this assumption as has been realized in our previous works and also in the present one (see below).

Now, each observed PDF $\hat{\Pi}^{(n)}(\xi_n)$ is symmetrized with respect to $\xi_n^{\rm peak}$, at which PDF has its peak value, by averaging the part $\xi_n \geq \xi_n^{\rm peak}$ and the part $\xi_n \leq \xi_n^{\rm peak}$. The value $\xi_n^{\rm peak}$ is positive for positively skewed PDF. After the symmetrization, we shift the horizontal position of the symmetrized PDF by putting $\xi_n^{\rm peak}$ as the origin of the horizontal axis. However, for the present analyses in this paper, each PDF is symmetrized at $\xi_n = 0$, since the peak points of the extracted PDFs locate between $\xi_n = 0$ and the next data point in the positive ξ_n axis. In order to do the proper symmetrization, we need more data points especially for the center part of the PDF.

The PDF for the energy transfer rates is given by the formulae in subsection 4.2 with $\phi = 3$. We put for $\hat{\Pi}^{(n)}_{\phi,{\rm cr}}(\xi_n)$ in (77) the trial function

$$\mathrm{e}^{-g_3(\xi_n)} = \left\{1 - \left(1-q'\right)\left[1 + f'(\alpha^*)\right]\left[(\xi_n/\xi_n^*)^w - 1\right]/w\right\}^{1/(1-q')} \tag{92}$$

of the Tsallis-type just because it can cover various shapes by changing the single parameter q'.[1] For example, it reduces to exponential function for $q' \to 1$, and to a Lorentzian shape for $q' = 2$ with respect to the variable $(\xi_n/\xi_n^\star)^{w/2}$. The parameters q' and w are adjusted by the property of the experimental PDFs near $\xi_n = 0$ with the theoretical formula for the PDF $\hat{\Pi}^{(n)}_{\phi}(\xi_n)$. The paremeter q' is tuned by adjusting the peak height of PDF at the center, i.e., at $\xi_n = 0$. Throughout the following analyses in this paper, the parameter w is settled to $w = 1.20$.

The PDFs of energy transfer rates by DNS are analyzed in Fig. 1, Fig. 2 and

[1]This parameter is another entropy index different from q in (45).

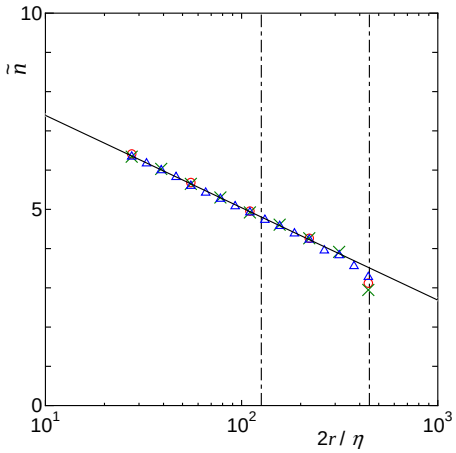

Figure 4. The relation between $\tilde{n}$ and $2r/\eta$ extracted from the PDFs of energy transfer rates for $\delta = 2^{1/4}$ (open triangles), for $\delta = 2^{1/2}$ (crosses; the series A in Table 1) and for $\delta = 2$ (open circles; the series A in Table 1). The line is $\tilde{n} = -1.02\ln(2r/\eta) + 9.75$. Here, $2r$ corresponds to ℓ_n. Note that the inertial range is the region between the vertical dash-dotted lines.

Fig. 3, respectively, for the magnifications $\delta = 2^{1/4}$, $\delta = 2^{1/2}$ and $\delta = 2$ on (a) log and (b) linear scale in the vertical axes. For better visibility, each PDF is shifted by appropriate unit along the vertical axis. Open circles in the figures are the DNS data points for PDF. The profiles of the PDF are shown only the part of their right-hand side. Solid lines represent the theoretical PDFs given in subsection 4.2 with $\phi = 3$.

Through the analyses, it turns out that the turbulent system under consideration is characterized with the value $\mu = 0.320$ for the intermittency exponent. Then, the parameters necessary for the PDF within A&A model are determined as $(1-q)\ln\delta = 0.323$, $\alpha_0 = 1.19$ and $X = 0.382$, which are independent of δ. The entropy indexes become $q = -0.862$ for $\delta = 2^{1/4}$ $(= 1.19)$, $q = 0.068$ for $\delta = 2^{1/2}$ $(= 1.41)$ and $q = 0.534$ for $\delta = 2$. Other parameters extracted by the analyses of the PDFs from DNS with the theoretical PDFs are listed in Table 1 for each δ. There are two distinct series of observations A and B for the magnification $\delta = 2^{1/2}$, whereas there are four distinct series A, B, C and D for $\delta = 2$.

The dependences of the values of $\tilde{n}$ on $2r/\eta = \ell_n/\eta$, listed in Table 1, are shown in Fig. 4. The formulae for the dependences are extracted by the method of least squares for $\delta = 2^{1/4}$, $\delta = 2^{1/2}$ and $\delta = 2$ as

$$\tilde{n} = -1.02\ln(2r/\eta) + 9.72, \tag{93}$$

$$\tilde{n} = -1.03\ln(2r/\eta) + 9.76, \tag{94}$$

$$\tilde{n} = -1.02\ln(2r/\eta) + 9.78, \tag{95}$$

respectively. Here, the Kolmogorov scale η for the DNS [30] is $\eta = 5.12 \times 10^{-4}$. Since these formulae are almost common for every δ, we draw in Fig. 4 the line

$$\tilde{n} = -1.02\ln(2r/\eta) + 9.75 \tag{96}$$

for reference. This independence of δ proves the correctness of the conjecture that $\tilde{n}$ is independent of δ. From Fig. 4, we find the remarkable outcome that there exists a scaling behavior extended to smaller region from the inertial range that is the range between the vertical dash-dotted lines, i.e., $126 < 2r/\eta < 448$ [30]. This may be attributed to the fact that MPDFT is the theory looking at the singularities

Table 1. The values of δ and the parameters extracted in the course of theoretical analyses. For magnification $\delta = 2^{1/2}$, there is two distinct series of observations A and B. For $\delta = 2$, there is four distinct series A, B, C and D. The parameter w is settled to 1.20 throughout the analysis.

	$\delta = 2^{1/4}$					$\delta = 2^{1/2}$						$\delta = 2$					
$2r/\eta$	n	$\tilde{n}$	q'	α^*	ξ_n^*	series	n	$\tilde{n}$	q'	α^*	ξ_n^*	series	n	$\tilde{n}$	q'	α^*	ξ_n^*
27.5	36.6	6.34	0.320	0.964	0.373	A	18.3	6.34	0.460	0.954	0.393	A	9.25	6.41	0.653	0.930	0.438
32.8	35.6	6.17	0.200	0.963	0.381	B	17.9	6.20	0.410	0.954	0.401	B	9.00	6.24	0.600	0.930	0.448
38.9	34.6	6.00	0.172	0.963	0.293	A	17.4	6.03	0.350	0.954	0.412	C	8.78	6.09	0.560	0.930	0.459
46.3	33.6	5.82	0.330	0.963	0.411	B	16.8	5.82	0.500	0.954	0.433	D	8.50	5.89	0.650	0.930	0.479
55.1	32.3	5.60	0.600	0.964	0.443	A	16.3	5.65	0.510	0.954	0.448	A	8.20	5.68	0.678	0.930	0.496
65.6	31.3	5.42	0.530	0.963	0.454	B	15.8	5.47	0.550	0.953	0.466	B	7.90	5.48	0.730	0.930	0.517
78.0	30.4	5.27	0.520	0.963	0.468	A	15.3	5.30	0.550	0.954	0.480	C	7.70	5.34	0.685	0.930	0.527
92.7	29.3	5.08	0.530	0.963	0.486	B	14.8	5.11	0.580	0.954	0.500	D	7.45	5.16	0.660	0.930	0.542
110	28.4	4.92	0.440	0.962	0.496	A	14.2	4.92	0.568	0.954	0.518	A	7.15	4.96	0.658	0.930	0.562
131	27.3	4.73	0.540	0.963	0.523	B	13.8	4.77	0.530	0.954	0.532	B	7.00	4.85	0.600	0.930	0.569
156	26.4	4.58	0.433	0.963	0.533	A	13.3	4.61	0.400	0.954	0.541	C	6.70	4.64	0.535	0.930	0.587
185	25.3	4.38	0.540	0.963	0.562	B	12.6	4.35	0.550	0.954	0.579	D	6.50	4.51	0.500	0.930	0.600
221	24.4	4.23	0.350	0.963	0.569	A	12.3	4.26	0.350	0.954	0.578	A	6.15	4.26	0.450	0.930	0.620
264	22.8	3.95	0.300	0.960	0.600	B	11.4	3.95	0.460	0.954	0.623	B	5.75	3.99	0.534	0.930	0.659
314	22.1	3.83	0.450	0.963	0.628	A	11.3	3.92	0.320	0.954	0.631	C	5.60	3.88	0.337	0.930	0.664
374	20.5	3.55	0.500	0.961	0.672	B	9.10	3.15	0.710	0.943	0.765	D	5.00	3.47	0.480	0.930	0.727
442	18.0	3.28	1.00	0.956	0.687	A	8.50	2.95	0.550	0.945	0.761	A	4.50	3.12	0.450	0.930	0.766

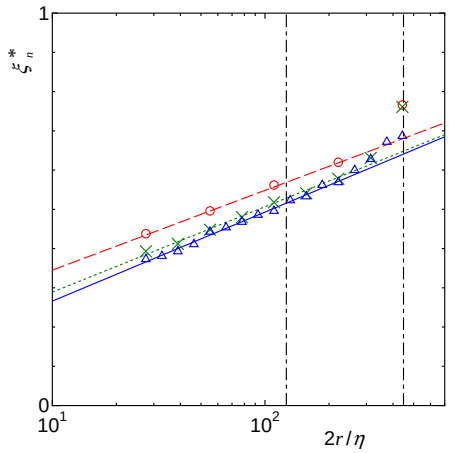

Figure 5. The relation between ξ_n^* and $2r/\eta$ extracted from the PDFs of energy transfer rates for $\delta = 2^{1/4}$ (open triangles), for $\delta = 2^{1/2}$ (crosses; the series A in Table 1) and for $\delta = 2$ (open circles; the series A in Table 1). The solid line, the dotted line and the dashed line are, respectively, $\xi_n^* = 0.0986\ln(2r/\eta)+0.0392$, $\xi_n^* = 0.0945\ln(2r/\eta)+0.0714$ and $\xi_n^* = 0.0883\ln(2r/\eta)+0.142$. Here, $2r$ correspond to ℓ_n. Note that the inertial range is the region between the vertical dash-dotted lines.

which become more conspicuous as $2r$ $(= \ell_n)$ getting smaller (see the discussion in section 2). Note that the scaling behavior breaks near the larger end of the inertial range.

The comparison of the extracted formula (96) for $\tilde{n}$ with the theoretical relation

$$\tilde{n} = -\ln(2r/\eta) + \ln(\ell_0/\eta) \tag{97}$$

provides us with the estimation $\ell_0/\eta = 1.72 \times 10^4$. Since the smallest grid spacing is 3η [30], $\ell_0/3\eta = 5.72 \times 10^3$ provides us with the number of grids corresponding to ℓ_0. Note that the estimated value of $\ell_0/3\eta$ is about 2.8 times larger than the possible largest meaningful length 2048 in the unit of the number of grids due to the periodic boundary condition of the DNS. Note also that ℓ_0/η is about 8 times larger than the integral length $L/\eta = 2.130 \times 10^3$ of the DNS under consideration [30].

The values α^* of the connection point are almost constant with respect to $2r/\eta$, but they depend slightly on δ (see Table 1). The corresponding values for the connection point ξ_n^* are given by (78) with (72) and (89) for $\phi = 3$, and are listed in Table 1. The dependence of ξ_n^* on $2r/\eta$ is extracted out by the method of least squares in the forms

$$\xi_n^* = 0.0986\ln(2r/\eta) + 0.0392, \tag{98}$$

$$\xi_n^* = 0.0945\ln(2r/\eta) + 0.0714, \tag{99}$$

$$\xi_n^* = 0.0883\ln(2r/\eta) + 0.142, \tag{100}$$

respectively, for $\delta = 2^{1/4}$, $\delta = 2^{1/2}$ and $\delta = 2$. These lines are drawn in Fig. 5. It is remarkable that the extracted formula has rather simple form in spite of the fact that ξ_n^* has a complicated dependence on $2r/\eta$ due to the implicit dependences through the quantities (72) and (89) in addition to the explicit dependence in (78). It is also remarkable that the connection point ξ_n^* has a scaling behavior extended to smaller region from the inertial range which is the region between the vertical dash-dotted lines [30].

The entropy index q' of the PDFs ($\phi = 3$) for the central part (83) with (92) for $\delta = 2^{1/4}$, $\delta = 2^{1/2}$ and $\delta = 2$ are plotted in Fig. 6. Although the values of q' locate around 0.5, they are scattered for the present analyses of the energy transfer

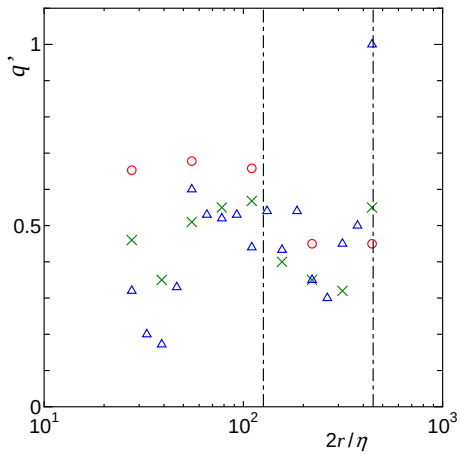

Figure 6. The relation between q' and $2r/\eta$ extracted from the PDFs of energy transfer rates for $\delta = 2^{1/4}$ (open triangles), for $\delta = 2^{1/2}$ (crosses) and for $\delta = 2$ (open circles). Note that the inertial range is the region between the vertical dash-dotted lines.

rates. The cause of the scattered values of q' and of the sharp peak at $\xi_n = 0$ may be attributed to the inappropriate symmetrization of the experimental PDFs. We expect that, with the analyses near the center part of PDFs based on more data points and with the appropriate symmetrization of PDFs, one can extract the more reasonable characteristics of fluctuations around the coherent turbulent motion. The results of the reexamination in this direction will be published elsewhere in the near future.

6. Summary and Prospects

We showed successfully the validity of the scaling relation (3) in a high accuracy through the analyses of the PDFs for energy transfer rates, extracted out from 4096^3 DNS [30] with the magnification $\delta = 2^{1/4}$. As the value δ (> 1) is chosen arbitrarily by observers when they produce a series of PDFs, observables of a turbulent system should not depend on δ. From the original series, we created two more series with magnifications $\delta = 2^{1/2}$ and $\delta = 2$ in order to check if the choice of δ does not affect observables of the turbulent system under the analysis by MPDFT with the new scaling relation. Here, observables are the multifractal spectrum, the mass exponents, the scaling exponents and so on. The independence of observables on δ has been proven through the accurate analyses of PDFs performed in this paper (see Fig 1, Fig. 2 and Fig. 3). It is also revealed that $\tilde{n}$ does not depend on δ, which ensures the uniqueness of the PDF of α for any value of δ.

It is found from the dependence of $\tilde{n}$ on $2r$ ($= \ell_n$) that the scaling behavior extends itself to smaller region with respect to $2r$ than the inertial range (see Fig. 4). It is reasonable in the sense that MPDFT is the formalism analyzing the singularities of those observables responsible for intermittency which is important for smaller ℓ_n. The dependence of the connection point ξ_n^* on $2r$ also shows a scaling behavior extended to smaller region than the inertial range (see Fig. 5), although the scaling relation has a slight dependence on δ which may be attributed to the fact that the lack of data points for the center part of PDF. The reconsideration of this point accompanied by the refinement to the scattered q' values is in progress and will be reported elsewhere in the near future. The information of the connection point ξ_n^* may be useful for the analyses by wavelet [33–36] and curvelet [37, 38] to separate the coherent motion of eddies in turbulence and the fluctuation around

eddies.

It is revealed that α^* at the connection point are constant with respect to $2r$ for each δ, but its value depends slightly on δ. In this paper, we adjusted the connection point α^*, therefore ξ_n^*, in order for the best fit of the PDF around the point. In the previous analyses, we had chosen the connection point under the criterion that the PDF $\hat{\Pi}_\phi^{(n)}(\xi_n^*)$ at the connection point should have the least dependence on n. The values $\alpha_{\rm old}^*$ thus determined are also constant with respect to $2r$, but are different from the values α^* extracted through the adjustment performed in the present paper. The difference between the values α^* and $\alpha_{\rm old}^*$ is quite small. For the case of the PDFs for energy transfer rates with $\delta = 2$ investigated in this paper, $\alpha^* = 0.930$ (see Table 1) and $\alpha_{\rm old}^* = 0.928$. Note that the previous analyses had been done only for $\delta = 2$.

The precise verification of the scaling relation (3), as was done in the present paper, is essential to provide a new interpretation of turbulence since we observe that the scaling relation is intimately related to a δ-scale Cantor set associated with unstable δ^∞ periodic orbits. We expect that the present work opens a door to the route for deeper understanding of the role of the Tsallis-type distribution function, and that its goal can be found by a further investigation on the properties of the unstable δ^∞ periodic orbits. The new scaling relation proposed in this paper is related to the one extracted in a dynamical system, say the system of logistic map. Then, we observe that the origin of the multifractal character of the fully developed turbulence is deeply related to the δ-scale Cantor sets created from δ^∞ periodic orbits. From the present analyses, we conjecture that the system of the fully developed turbulence consists of the accumulation of the Cantor sets characterized by unstable δ^∞ periodic orbits with different values of δ. Observation of the system with the magnification δ extracts the information of the δ-scale Cantor sets constituting the turbulence. Further investigations to this direction is now in progress, and will be given elsewhere in the near future.

Acknowledgements

The authors are grateful to Dr. Y. Kaneda and Dr. T. Ishihara for their kindness to provide them with the PDF data for the energy transfer rates extracted out from their 4096^3 DNS of fully developed turbulence. They also thank to Dr. T. Motoike, Dr. K. Yoshida, Mr. M. Komatsuzaki and Mr. K. Takechi for fruitful discussions.

References

[1] B.B. Mandelbrot, *Intermittent turbulence in self-similar cascades: divergence of high moments and dimension of the carrier*, J. Fluid Mech. 62 (1974), pp. 331–358.
[2] U. Frisch, and G. Parisi, *Turbulence and predictability in geophysical fluid dynamics and climate dynamics*, M. Ghil, R. Benzi and G. Parisi, eds., North-Holland, New York, 1985, pp. 84–88.
[3] R. Benzi, G. Paladin, G. Parisi, and A. Vulpiani, *On the multifractal nature of fully developed turbulence and chaotic systems*, J. Phys. A: Math. Gen. 17 (1984), pp. 3521–3531.
[4] T.C. Halsey, M.H. Jensen, L.P. Kadanoff, I. Procaccia, and B.I. Shraiman, *Fractal measures and their singularities: The characterization of strange sets*, Phys. Rev. A 33 (1986), pp. 1141–1151.
[5] C. Meneveau, and K. R. Sreenivasan, *The multifractal spectrum of the dissipation field in turbulent flows*, Nucl. Phys. B (Proc. Suppl.) 2 (1987), pp. 49–76.
[6] M. Nelkin, *Multifractal scaling of velocity derivatives in turbulence*, Phys. Rev. A 42 (1990), pp. 7226–7229.
[7] I. Hosokawa, *Turbulence models and probability distributions of dissipation and relevant quantities in isotropic turbulence*, Phys. Rev. Lett. 66 (1991), pp. 1054–1057.
[8] R. Benzi, L. Biferale, G. Paladin, A. Vulpiani, and M. Vergassola, *Multifractality in the statistics of the velocity gradients in turbulence*, Phys. Rev. Lett. 67 (1991), pp. 2299–2302.
[9] Z-S. She, and E. Leveque, *Universal scaling laws in fully developed turbulence*, Phys. Rev. Lett. 72 (1994), pp. 336–339.

[10] T. Arimitsu, and N. Arimitsu, *Analysis of fully developed turbulence in terms of Tsallis statistics*, Phys. Rev. E 61 (2000), pp. 3237–3240.
[11] T. Arimitsu, and N. Arimitsu, *Tsallis statistics and fully developed turbulence*, J. Phys. A: Math. Gen. 33 (2000), pp. L235–L241. [CORRIGENDUM: 34 (2001), pp. 673–674.]
[12] N. Arimitsu, and T. Arimitsu, *Multifractal Analysis of Turbulence by Statistics based on Non-Extensive Tsallis' or Extensive Renyi's Entropy*, J. Korean Phys. Soc. 40 (2002), pp. 1032–1036, and the references therein.
[13] T. Arimitsu, and N. Arimitsu, *PDF of velocity fluctuation in turbulence by a statistics based on generalized entropy*, Physica A 305 (2002), pp. 218–226.
[14] L. Biferale, G. Boffetta, A. Celani, B.J. Devenish, A. Lanotte, and F. Toschi, *Multifractal statistics of Lagrangian velocity and acceleration in turbulence*, Phys. Rev. Lett. 93 (2004), pp. 064502-1-4.
[15] T. Arimitsu, and N. Arimitsu, *Multifractal analysis of various PDF in turbulence based on generalized statistics: A way to tangles in superfluid He*, AIP Conf. Proc. 695 (2003), pp. 135–144.
[16] T. Arimitsu, and N. Arimitsu, *Multifractal analysis of fluid particle accelerations in turbulence*, Physica D 193 (2004), pp. 218–230.
[17] T. Gotoh and R.H. Kraichnan, *Turbulence and Tsallis statistics*, Physica D 193 (2004) pp. 231–244.
[18] T. Arimitsu, and N. Arimitsu, *Harmonious representation of PDF's reflecting large deviations*, Physica A 340 (2004), pp. 347–355.
[19] T. Arimitsu, and N. Arimitsu, *Multifractal analysis of the fat-tail PDFs observed in fully developed turbulence*, Journal of Physics: Conference Series 7 (2005), pp. 101–120.
[20] L. Chevillard, B. Castaing, E. Lévêque and A. Arneodo, *Unified multifractal description of velocity increments statistics in turbulence: Intermittency and skewness*, Physica D 218 (2006), pp. 77-82.
[21] T. Arimitsu, N. Arimitsu, K. Yoshida, and H. Mouri, *Multifractal PDF analysis for intermittent systems*, in *Anomalous Fluctuation Phenomena in Complex Systems: Plasma Physics, Bio-Science and Econophysics*, eds. C. Riccardi and H.E. Roman, Research Signpost, India, 2008, pp. 25–55; and the references therein.
[22] A.M. Oboukhov, *Some specific features of atmospheric turbulence*, J. Fluid Mech. 13 (1962), pp. 77–81.
[23] A.N. Kolmogorov, *A refinement of previous hypotheses concerning the local structure of turbulence in a viscous incompressible fluid at high Reynolds number*, J. Fluid Mech. 13 (1962), pp. 82–85.
[24] A.M. Yaglom, *The influence of fluctuations in energy dissipation on the shape of turbulent characteristics in the inertial interval*, Sov. Phys. Dokl. 11 (1966), pp. 26–29.
[25] U.M.S. Costa, M.L. Lyra, A.R. Plastino, and C. Tsallis, *Power-law sensitivity to initial conditions within a logistic-like family of maps: Fractality and nonextensivity*, Phys. Rev. E 56 (1997), pp. 245–250.
[26] M.L. Lyra, and C. Tsallis, *Nonextensivity and multifractality in low-dimensional dissipative systems*, Phys. Rev. Lett. 80 (1998), pp. 53–56.
[27] A. Rényi, *On measures of entropy and information*, in *Proceedings of the 4th Berkeley Symposium on Mathematical Statistics and Probability*, Berkeley, USA, 20 June–30 July 1961, Univ. of California Press, Berkeley, 1961, pp. 547–561.
[28] J.H. Havrda, and F. Charvat, *Quantification methods of classification processes: Concepts of structural α entropy*, Kybernatica 3 (1967), pp. 30–35.
[29] C. Tsallis, *Possible generation of Boltzmann-Gibbs statistics*, J. Stat. Phys. 52 (1988), pp. 479–487.
[30] T. Aoyama, T. Ishihara, Y. Kaneda, M. Yokokawa, K. Itakura, and A. Uno, *Statistics of energy transfer in high-resolution direct numerical simulation of turbulence in a periodic box*, J. Phys. Soc. Jpn. 74 (2005) pp. 3202–3212.
[31] A.N. Kolmogorov, *The local structure of turbulence in incompressible viscous fluid for very large Reynolds numbers*, Dokl. Akad. Nauk. SSSR 30 (1941), pp. 301–305.
[32] A.N. Kolmogorov, *Dissipation of energy in locally isotropic turbulence*, Dokl. Akad. Nauk. SSSR 31 (1941), pp. 538–540.
[33] M. Farge, *Wavelet transforms and their applications to turbulence* Annu. Rev. Fluid Mech. 24 (1992), pp. 395–457.
[34] M. Yamada and K. Ohkitani, *An idenfication of energy cascade in turbulence by orthonormal wavelet analysis*, Prog. Theor. Phys. 86 (1991), pp. 799–815.
[35] C. Meneveau, *Analysis of turbulence in the orthonormal wavelet representation*, J. Fluid Mech. 232 (1991), pp. 469–520.
[36] H. Mouri, H. Kubotani, T. Fujitani, H. Niino and M. Takaoka, *Wavelet analyses of velocities in laboratory isotropic turbulence*, J. Fluid Mech. 389 (1999), pp. 229–254.
[37] J. Ma, M.Y. Hussaini, O.V. Vasilyev and F.-X. Le Dimet, *Multiscale geometric analysis of turbulence by curvelet*, Phys. Fluids 21 (2009), pp. 075104-1–19.
[38] I. Bermejo-Moreno and D. Pullin, *On the non-local geometry of turbulence*, J. Fluid Mech. 603 (2008), pp. 101–135.